

BLUE COMPACT DWARF GALAXIES WITH SPITZER: THE INFRARED/RADIO PROPERTIES

YANLING WU¹, V. CHARMANDARIS^{2,3}, J. R. HOUCK¹, J. BERNARD-SALAS¹, V. LEBOUTELLER¹, B. R. BRANDL⁴, D. FARRAH¹

Accepted by ApJ, November 27th, 2007

ABSTRACT

We study the correlation between the radio, mid-infrared and far-infrared properties for a sample of 28 blue compact dwarf (BCD) and low metallicity star-forming galaxies observed by *Spitzer*. We find that these sources extend the same far-infrared to radio correlation typical of star forming late type galaxies to lower luminosities. In BCDs, the 24 μ m (or 22 μ m) mid-infrared to radio correlation is similar to starburst galaxies, though there is somewhat larger dispersion in their q_{24} parameter compared to their q_{FIR} . No strong correlations between the q parameter and galaxy metallicity or effective dust temperature have been detected, though there is a hint of decreasing q_{24} at low metallicities. The two lowest metallicity dwarfs in our sample, IZw18 and SBS0335-052E, despite their similar chemical abundance, deviate from the average q_{24} ratio in opposite manners, displaying an apparent radio excess and dust excess respectively.

Subject headings: galaxies:starburst — galaxies: dwarf — infrared: galaxies — radio continuum: galaxies

1. INTRODUCTION

More than 35 years ago, a correlation between the 10 μ m mid-infrared (mid-IR) and 1.4 GHz luminosities in galactic nuclei was first noticed by van der Kruit (1971). In 1983, the launch of the *Infrared Astronomical Satellite (IRAS)* brought a new era in collecting large samples of data in the infrared, and sparked numerous studies investigating the above mentioned correlation in star forming galaxies. Both the radio and infrared emission are closely related to star formation activities. The radio continuum is known to originate from two processes: thermal free-free emission from ionized gas in HII regions and non-thermal synchrotron radiation from relativistic electrons that are accelerated in the supernovae remnants (SNRs) (see Condon 1992, for a review). The thermal emission usually has a rather flat spectrum with $f_\nu \propto \nu^{-0.1}$ while the non-thermal component often has a much steeper spectral slope with $f_\nu \propto \nu^{-0.8}$. In normal galaxies the relative contribution of the two components varies with frequency and at 1.4 GHz the radio continuum is dominated (at nearly $\sim 90\%$) by the non-thermal component. The infrared emission is due to the thermal re-radiation of starlight from dust surrounding HII regions (Harwit & Pacini 1975). Based mostly on *IRAS* data, it has been shown that the far-infrared (FIR, 40-120 μ m) to radio correlation holds well over a remarkably wide range of star forming galaxies, spanning several orders of magnitude in luminosities (Helou et al. 1985; de Jong et al. 1985; Condon et al. 1991; Yun et al. 2001). The availability of deep observations of distant galaxies by the *Infrared Space Observatory (ISO)* and

recently by *Spitzer* (Werner et al. 2004) showed that the correlation between the IR and radio emission is not limited to the local universe but also extends in galaxies at higher redshifts (Garrett 2002; Appleton et al. 2004). It was also revealed that in addition to the FIR, the mid-IR emission at $\sim 24\mu$ m correlates with the 20cm radio continuum, though with more scatter (Elbaz et al. 2002; Gruppioni et al. 2003; Appleton et al. 2004; Wu et al. 2005). A number of very deep *Spitzer* mid-IR and FIR surveys can now probe a population of galaxies with low infrared luminosities for which ancillary data, including deep radio imaging, are becoming available (e.g. Jannuzi & Dey 1999; Sanders et al. 2007; Rosenberg et al. 2006). This is particularly interesting since in the near future $\sim 20\mu$ m is the longest wavelength which will likely be probed by the James Web Space Telescope. It is thus instructive to examine the mid-IR to radio correlation in more detail in these low luminosity nearby systems, for which little is known to date.

As ubiquitous as the FIR/radio correlation appears to be, there are a few significant deviations from it. Radio excess exists in some instances, such as galaxies hosting an active galactic nucleus (AGN). External magnetic field compression due to the interaction with nearby galaxies could also produce extra emission in the radio continuum (Miller & Owen 2001). Conversely, synchrotron deficiency has been found in some nascent starburst galaxies studied by Roussel et al. (2003, 2006) which was attributed to the lack of time for massive young stars to evolve into supernovae (SN) since these galaxies are just at the onset of a starburst episode. On the other hand, as discussed in the infrared, dust emission can be damped in an optically-thin environment, because the ultraviolet (UV) and optical light may not be fully reprocessed by the dust, as seen in low luminosity dwarf galaxies.

Blue compact dwarf galaxies are a group of extragalactic objects that are characterized by their blue op-

Electronic address: wyl@astro.cornell.edu, vassilis@physics.uoc.gr, jrh13@cornell.edu, jbs1@cornell.edu, vlad@astro.cornell.edu, brandl@str

¹ Astronomy Department, Cornell University, Ithaca, NY 14853

² University of Crete, Department of Physics, GR-71003, Heraklion, Greece

³ IESL/Foundation for Research and Technology - Hellas, GR-71110, Heraklion, Greece and Chercheur Associé, Observatoire de Paris, F-75014, Paris, France

⁴ Leiden Observatory, Leiden University, P.O. Box 9513, 2300 RA Leiden, The Netherlands

tical colors, small sizes (≤ 1 kpc) and low luminosities ($M_B > -18$). These galaxies do not display any AGN signature⁵ and have recent bursts of star formation in a relatively unevolved chemical environment. As such they have been proposed as nearby analogs of star formation in young galaxies in the early universe. In a metal poor environment, star forming regions are usually optically thin and emit less in the infrared. However, Devereux & Eales (1989) suggested that in a low luminosity galaxy, the radio emission also decreases, and probably faster than the infrared. The deficiency in both the non-thermal radio and FIR emission may counterbalance each other and result in a similar FIR/radio ratio to the one observed in normal spiral galaxies (Klein et al. 1991). This was examined by a study of star formation rates (SFRs) in BCDs performed by Hopkins et al. (2002), in which the authors found an excellent agreement between the SFRs estimated from 1.4 GHz and 60 μ m luminosities. As Bell (2003) has pointed out though, the FIR/radio correlation is almost linear, not because the IR and radio emission reflect the SFRs correctly, but because in low luminosity galaxies they are both underestimated by similar factors. This is in agreement with Helou & Bicay (1993), who found from their modelling work in disk galaxies that the transparency of the disk was about the same to both re-emission processes. Hunt et al. (2005a) in their analysis of the spectral energy distributions (SEDs) of low metallicity BCDs, noticed that these systems do not follow several of the usual correlations between the mid-IR, FIR and radio emission and display a scatter of a factor of ~ 10 .

The *Spitzer* Space telescope has enabled us to study the infrared properties of a large sample of BCDs, probing the lower end of the luminosity and metallicity range. In this paper, the fifth in a series (Houck et al. 2004b; Wu et al. 2006, 2007a,b), we examine their mid-IR and FIR to radio correlation extending the work of Hopkins et al. (2002). We describe the sample selection and the observational data in §2. A detailed study of mid-IR and FIR/radio correlation, as well as its dependence with other parameters, such as metallicity and dust temperature are presented in §3. We also discuss two extreme cases, IZw18 and SBS0335-052 in §3. We summarize our conclusions in §4.

2. OBSERVATIONS

As part of the IRS⁶ (Houck et al. 2004a) Guaranteed Time Observation (GTO) program (PID: 85), we have compiled a sample of BCD candidates (~ 64) selected from the Second Byurakan Survey (SBS), Bootes void galaxies (Kirshner et al. 1981; Popescu & Hopp 2000), and other commonly studied BCDs. These sources are known to have low metallicities ranging from $0.03 Z_{\odot}$ to $0.5 Z_{\odot}$ ⁷. Their 22 μ m fluxes have been published

⁵ A possible exception among our sources is CG0752 in which the high ionization lines [NeV] λ 14.3/24.3 μ m are detected (see Hao et al. 2007).

⁶ The IRS was a collaborative venture between Cornell University and Ball Aerospace Corporation funded by NASA through the Jet Propulsion Laboratory and the Ames Research Center.

⁷ Here we adopt the new oxygen solar abundance of $12 + \log(O/H) = 8.69$ (Allende Prieto et al. 2001). Wu et al. (2007b) have derived neon and sulfur abundances for a sample of BCDs using the infrared data, but these abundances are not available for all of the sources in this study.

in Wu et al. (2006). We also include 10 galaxies from Engelbracht et al. (2005) (PID: 59), which are mostly BCDs and starburst galaxies, and span a larger metallicity range ($0.03 Z_{\odot} \sim 1.5 Z_{\odot}$)⁸. For all galaxies with 22 (24) μ m detections, we searched the literature as well as the public archives (NVSS and FIRST) for 1.4 GHz radio continuum data. We restrict our sample to sources with both mid-IR and radio detections which results in a sample of 23 galaxies. Finally, we also include 5 galaxies that have 22 μ m detections and 1.4 GHz upper limits published by Hopkins et al. (2002) for comparison between ours and Hopkins' samples. Note that the sample was not selected based on infrared properties, but merely on BCD-type objects and the availability of both infrared and radio data. As a result, our sample is not complete, but the large number of sources that only became detectable in the infrared with *Spitzer*, allows us to probe the properties of low luminosity dwarf galaxies, and provide statistically meaningful results. The observational information for this sample and previously published data are presented in Table 1, which includes the positions of the sources, their mid-IR, FIR and 1.4 GHz flux densities, as well as oxygen abundances of the ionized gas.

All sources in this study have mid-IR flux measurements either at 22 μ m with the IRS red peak-up camera and/or at 24 μ m with MIPS (Rieke et al. 2004). The photometric fluxes of these two bands differ by less than 10% for galaxies in the local universe. This was confirmed by using a suite of ~ 100 spectra of nearby galaxies from our IRS/GTO database and calculating their synthetic 22 and 24 μ m fluxes after convolving the spectra with the corresponding filter response curves. For consistency, in our analysis we use the MIPS 24 μ m measurements, and the 22 μ m values are only used when the 24 μ m values are not available. For sources above the IRS 22 μ m and MIPS 24 μ m saturation limits we use the IRS low resolution spectrum to estimate a synthetic 24 μ m flux. We also obtained far-infrared fluxes for our sample from the archival *IRAS* 60 and 100 μ m data (Moshir & et al. 1990; Sanders et al. 2003).

Most of the 1.4 GHz radio continuum data are from the NRAO VLA Sky Survey (NVSS) (Condon et al. 1998), while one is from the Faint Images of the Radio Sky at Twenty cm (FIRST) (Becker et al. 1995), along with some individual observations (references in Table 1). A total of seven sources were too faint and were not included in the NVSS catalogue. For those we used the values of Hopkins et al. (2002) who studied a similar BCD sample and remeasured the 1.4 GHz fluxes using the images from NVSS and FIRST, providing radio detections for 2 sources and better upper limits for another five sources that overlaps with the galaxies in our sample.

Our final sample consists of 28 galaxies, all of which have *Spitzer* mid-IR 24 μ m and/or 22 μ m flux measurements. Among these galaxies, 23 sources have 1.4 GHz radio continuum data and 5 have measured upper limits. *IRAS* 60 μ m and 100 μ m fluxes are available for 16 sources and 3 more are detected only at 60 μ m. We list

⁸ The galaxies in PID 59 partly overlap with the BCDs in PID 85. We have also excluded some galaxies which the authors derived their 24 μ m fluxes by doing a color correction to the *IRAS* 25 μ m fluxes because of the aperture difference between these two band filters.

TABLE 1
PROPERTIES OF THE SAMPLE

ID	Object Name	RA J2000	Dec J2000	Flux (mJy)				12+log(O/H)	References			
				1.4 GHz	24(22) μ m	60 μ m	100 μ m		1.4 GHz	24 μ m	IRAS	Z
1	Haro11	00h36m52.5s	-33d33m19s	26.8	1900	6880	5040	7.9	(1)	(2)	(3)	(4)
2	NGC1140	02h54m33.6s	-10d01m40s	23.6	316.6	3358	4922	8.5	(1)	(5)	(6)	(7)
3	SBS0335-052E	03h37m44.0s	-05d02m40s	0.46	66	7.3	(8)	(2)		(9)
4	NGC1569	04h30m47.0s	+64d50m59s	336.3	2991	54360	55290	8.2	(1)	(2)	(3)	(10)
5	IIZw40	05h55m42.6s	+03d23m32s	32.5	1500	6570	5270	8.1	(1)	(2)	(3)	(7)
6	UGC4274	08h13m13.0s	+45d59m39s	10.5	240	3236	6448	8.5	(1)	(2)	(6)	
7	He2-10	08h36m15.2s	-26d24m34s	83.8	4900	8.9	(1)	(2)		(11)
8	NGC2782	09h14m05.1s	+40d06m49s	124.5	960	9170	13760	8.8	(1)	(2)	(3)	(12)
9	NGC2903	09h32m10.1s	+21d30m03s	444.5	2200	60540	130430	9.3	(1)	(2)	(3)	(11)
10	I Zw18	09h34m02.0s	+55d14m28s	1.83	5.5	7.2	(13)	(2)		(9)
11	SBS0940+544	09h44m16.7s	+54d11m33s	<2.3	2.3	7.5	(14)	(5)		(15)
12	NGC3077	10h03m19.1s	+68d44m02s	29.0	1500	15900	26530	8.6	(1)	(2)	(3)	(16)
13	Mrk153	10h49m05.0s	+52d20m08s	4.0	29	280	<480	7.8	(1)	(2)	(6)	(17)
14	VIIZw403	11h27m59.9s	+78d59m39s	1.2	28	7.7	(18)	(2)		(9)
15	Mrk1450	11h38m35.6s	+57d52m27s	<2.0	48	279	<575	8.0	(14)	(2)	(6)	(7)
16	UM448	11h42m12.4s	+00d20m03s	32.6	560	4139	4321	8.0	(1)	(2)	(6)	(7)
17	UM461	11h51m33.3s	-02d22m22s	<2.6	30	7.8	(14)	(2)		(9)
18	UM462	11h52m37.3s	-02d28m10s	5.8	110	944	896	8.0	(1)	(2)	(6)	(9)
19	SBS1159+545	12h02m02.4s	+54d15m50s	<2.3	6.4	7.5	(14)	(5)		(19)
20	NGC4194	12h14m09.5s	+54d31m37s	100.7	3100	23200	25160	8.8	(1)	(2)	(3)	(16)
21	NGC4670	12h45m17.1s	+27d07m32s	13.7	210	2634	4470	8.2	(1)	(2)	(6)	(12)
22	SBS1415+437	14h17m01.4s	+43d30m05s	4.3	19.6	7.6	(14)	(5)		(9)
23	Mrk475	14h39m05.4s	+36d48m21s	<2.7	10.8	7.9	(14)	(5)		(9)
24	CG0563	14h52m05.7s	+38d10m59s	6.2	97.0	870	1900	8.7	(1)		(6)	
25	CG0752	15h31m21.3s	+47d01m24s	4.8	138.9	837	1059	...	(1)	(5)	(6)	
26	SBS1533+574	15h34m13.8s	+57d17m06s	4.2	53.4	257	405	8.1	(14)	(5)	(6)	(9)
27	Mrk1499	16h35m21.1s	+52d12m53s	1.5	33.8	256	617	8.1	(20)	(5)	(6)	(21)
28	Mrk930	23h31m58.3s	+28d56m50s	12.2	170	1245	<2154	8.1	(1)	(2)	(6)	(7)

REFERENCES. — (1) Condon et al. (1998), (2) Engelbracht et al. (2005), (3) Sanders et al. (2003), (4) Bergvall & Östlin (2002), (5) Wu et al. (2006), (6) Moshir et al. (1990), (7) Guseva et al. (2000), (8) Hunt et al. (2004), (9) Izotov & Thuan (1999), (10) Kobulnicky & Skillman (1997), (11) Kobulnicky & Johnson (1999), (12) Heckman et al. (1998), (13) Hunt et al. (2005a), (14) Hopkins et al. (2002), (15) Thuan & Izotov (2005), (16) Storchi-Bergmann et al. (1994), (17) Kunth & Joubert (1985), (18) Leroy et al. (2005), (19) Izotov & Thuan (1998), (20) FIRST catalog, (21) Shi et al. (2005)

the photometry of our sources in Table 1. The uncertainty in the 22 μ m or 24 μ m photometry is less than 5%. The *IRAS* 60 μ m and 100 μ m fluxes typically have less than a few percent of error, but could go up to $\sim 15\%$ for some of the fainter sources. The rms noise level for NVSS is ~ 0.5 mJy beam $^{-1}$.

3. RESULTS

3.1. Mid-IR and FIR to Radio Correlation in BCDs

The sensitivity and efficiency of the *Spitzer* Space Telescope has allowed us to probe the correlation between the mid-IR and radio luminosities for a large number of galaxies. Using the 24 μ m and 70 μ m MIPS imaging data of the First Look Survey, Appleton et al. (2004) have demonstrated the first direct evidence for the universality of the mid-IR/radio and FIR/radio correlation to $z \sim 1$. Wu et al. (2005) have also studied the mid-IR/radio correlation in a sample of star-forming galaxies and found that both the 8 μ m and 24 μ m luminosity are clearly correlated with the 1.4GHz radio luminosity. Their sample included only a few (3) dwarf galaxies and suggested that there may be a slope change for dwarf galaxies, which could be due to the lower dust-to-gas ratios and lower metallicities of the dwarfs. A detailed analysis of the spatial distribution of the infrared to radio correlation using *Spitzer* data on a sample of nearby late type spiral galaxies has been performed by Murphy et al. (2006a,b) in which the authors found that the ratio of the mid-IR

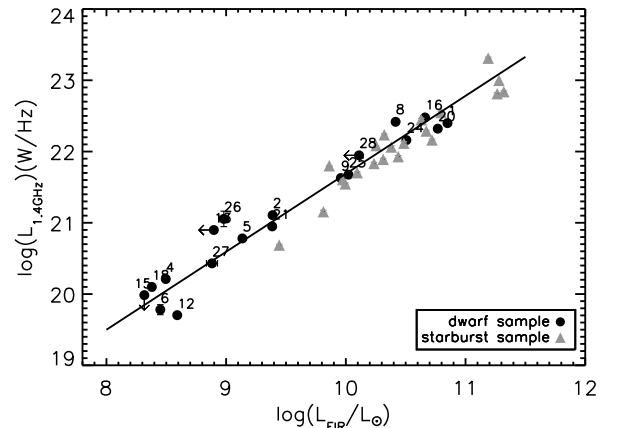


FIG. 1.— The FIR to 1.4 GHz radio luminosity correlation for this sample. Our data are presented with filled circles. The numbers next to each symbol correspond to their IDs in Table 1. The solid line is the best fit to this sample excluding the upper limits. For comparison, we have also include the starburst galaxies of Brandl et al. (2006), indicated with triangles.

and FIR to radio emission does vary from one region to the other. In general though, the dispersion is small and the ratio decreases with surface brightness and galactocentric radius.

Using the data from this sample of low metallicity dwarf galaxies we plot in Fig. 1 the radio luminos-

TABLE 2
DERIVED QUANTITIES OF THE SAMPLE

ID	Object Name	Distance ^a (Mpc)	L _{1.4GHz} ($\times 10^{20}$ W Hz ⁻¹)	L _{24μm} ($\times 10^8$ L _⊙)	L _{FIR} ($\times 10^8$ L _⊙)	q ₂₄	q _{FIR}
1	Haro11	88	250.5	584.2	706.3	1.85	2.46
2	NGC1140	21.2	12.8	5.6	24.4	1.13	2.29
3	SBS0335-052E	58	18.7	8.8	...	2.16	...
4	NGC1569	2.0	1.6	0.5	3.1	0.95	2.29
5	IIZw40	12.4	6.0	9.2	13.7	1.66	2.36
6	UGC4274	6.9	0.6	0.5	2.8	1.36	2.68
7	He2-10	12	15.6	29.9	...	1.77	...
8	NGC2782	41.7	216.3	66.3	260.4	0.89	2.00
9	NGC2903	8.9	42.5	6.9	90.9	0.69	2.34
10	IZw18	18.2	0.7	0.07	...	0.48	1.31 ^b
11	SBS0940+544	23	< 1.5	0.05	...	>0.00	...
12	NGC3077	3.8	0.5	0.9	3.9	1.71	2.89
13	Mrk153	40.5	7.9	1.9	<7.9	0.86	<2.00
14	VIIZw403	4.3	0.03	0.02	...	1.37	...
15	Mrk1450	20.0	<1.0	0.8	<2.1	>1.38	...
16	UM448	87.4	300.6	188.9	458.6	1.23	2.19
17	UM461	13.4	<0.6	0.2	...	>1.06	...
18	UM462	13.4	1.3	0.8	2.4	1.28	2.29
19	SBS1159+545	50	<7.0	0.6	...	>0.44	...
20	NGC4194	41.5	209.3	212.0	586.0	1.49	2.45
21	NGC4670	23.2	8.9	4.5	24.3	1.19	2.44
22	SBS1415+437	8.7	0.4	0.06	...	0.66	...
23	Mrk475	11.2	<0.4	0.05	...	>0.60	...
24	CG0563	139	144.6	74.4	320.5	1.19	2.35
25	CG0752	90	47.3	45.1	105.3	1.46	2.35
26	SBS1533+574	47	11.3	4.7	9.6	1.10	1.93
27	Mrk1499	39	2.7	2.0	7.6	1.35	2.46
28	Mrk930	77.5	88.4	40.5	<129.0	1.14	<2.17

^a The distances to the galaxies of the sample are adopted from Moustakas & Kennicutt (2006) when available, while the rest of the sources are calculated from the redshifts taken from NED, assuming a Λ CDM cosmology with $H_0 = 70$ km s⁻¹ Mpc⁻¹, $\Omega_m = 0.3$ and $\Omega_\lambda = 0.7$. For IZw18, we adopt the newly derived distance by Aloisi et al. (2007). The average uncertainty in the distances is $\sim 5\%$, mainly due to the value of H_0 .

^b This is calculated based on the “equivalent” *IRAS* 60 and 100 μ m fluxes (see Section 3.4).

ity of the sample as a function of the FIR luminosity. The luminosities of the sources we study span nearly 4 orders of magnitudes, but the correlation between the FIR and the radio is remarkably tight. The scatter in the ratio of the FIR and radio luminosities is 0.23 dex, i.e. less than a factor of 2. We performed a least-squares bisector fit to the data and found: $\log[L_{1.4\text{GHz}}(\text{WHz}^{-1})] = 1.09 \times \log(L_{\text{FIR}}/L_\odot) + 10.75$. For comparison, we have included in the plot the starburst galaxies from Brandl et al. (2006) marked with triangles, which has an identical slope (within 1σ). This slope of 1.09 ± 0.07 for the dwarf galaxy data agrees well with the slope of 1.10 ± 0.04 found by Bell (2003) for a sample of 162 galaxies, as well as the slope of 1.11 ± 0.02 for the infrared selected sources from the *IRAS* Bright Galaxy Sample (BGS) (Condon et al. 1991). This is also in agreement with Hopkins et al. (2002) and would suggest that globally our BCDs have a very similar FIR/radio correlation to normal galaxies.

Another way to parameterize the IR/radio correlation is to calculate the ratio of FIR to radio luminosity q_{FIR} according to the Helou et al. (1985) formula as well as the q_{24} following the definition of Appleton et al. (2004)⁹.

⁹ We use $q_{\text{FIR}} = \log[1.26 \times 10^{-14} (2.58S_{60\mu\text{m}} + S_{100\mu\text{m}}) / (3.75 \times 10^{12} F_{1.4\text{GHz}})]$ where $S_{60\mu\text{m}}$ and $S_{100\mu\text{m}}$ are in Jy and $F_{1.4\text{GHz}}$ is in $\text{Wm}^{-2}\text{Hz}^{-1}$ (Helou et al. 1985). We also define $q_{24} = \log(S_{24\mu\text{m}}/S_{1.4\text{GHz}})$ where $S_{24\mu\text{m}}$ and $S_{1.4\text{GHz}}$ are in Jy as in Appleton et al. (2004).

We plot the q_{24} values for our sample as a function of the 24 μ m luminosity of the galaxies in Fig. 2. For this sample we find that $q_{\text{FIR}} = 2.4 \pm 0.2$, consistent with the value of normal galaxies of $q_{\text{FIR}} = 2.3 \pm 0.2$ found by Condon (1992). When using the mid-IR 24 μ m data, we find that $q_{24} = 1.3 \pm 0.4$ (see Table 2). The standard deviation in q_{24} is \sim twice that of q_{FIR} . This is not unexpected given that the spectrum of star forming galaxies shows substantially larger variations in spectral slope in the mid-IR (see Brandl et al. 2006) than in the FIR (Dale et al. 2006). A small change in the geometry of the emitting regions would affect $F_\nu(24 \mu\text{m})$ and thus q_{24} ratio much more than the FIR emission and q_{FIR} . A similar result has also been noticed by Appleton et al. (2004) and Murphy et al. (2006a) who found a larger dispersion in q_{24} as compared to q_{70} ¹⁰ and suggested that this is probably due to a larger intrinsic dispersion in the IR/radio correlation at shorter wavelengths. Interestingly, the Appleton et al. (2004) values for $q_{24} = 0.84 \pm 0.28$ or the k-corrected q_{24} of 0.94 ± 0.23 are somewhat smaller than our results, though consistent within 2σ . One possible explanation is that the dust temperature of low luminosity dwarf galaxies tends to peak at shorter wavelength than normal star forming galaxies, which would result in an elevated 24 μ m based luminosity. An alternative explanation is that due to the peculiar morphology of dwarf

¹⁰ We define $q_{70} = \log(S_{70\mu\text{m}}/S_{1.4\text{GHz}})$ where $S_{70\mu\text{m}}$ and $S_{1.4\text{GHz}}$ are in Jy as in Appleton et al. (2004).

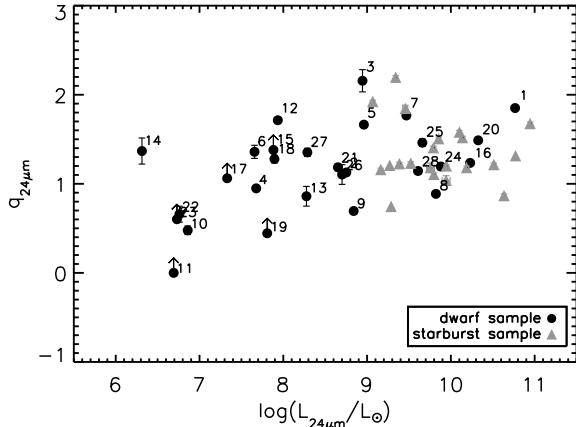


FIG. 2.— The q_{24} as a function of the the $24\mu\text{m}$ monochromatic luminosity L_{24} . The symbols are the same as in Fig. 1.

galaxies, more electrons escape from the galaxy because of the cosmic ray diffusion. Boyle et al. (2007) have also found a high $q_{24}=1.39\pm 0.02$ for the sources they studied, and postulated that this may be due to a change in the mean q_{24} ratio for objects with $F_{\nu}(24\mu\text{m}) < 1\text{ mJy}$, however, their sources are much further away and may not be comparable to the low metallicity star forming galaxies we study in the local universe.

3.2. Metallicity and Dust Temperature Effects on q_{IR}

A number of physical parameters, such as the metallicity, dust grain size distribution, and temperature may affect the shape of the infrared SED. Consequently, we search for correlations between the q ratios of the galaxies in our sample with those parameters. Our sample covers a metallicity range of $7.2 \leq 12 + \log(\text{O}/\text{H}) \leq 8.9$. In low metallicity galaxies, the dust content is usually low, even though there are notable exceptions such as SBS0335-052E (Houck et al. 2004b), thus the emission of UV light might not be fully reprocessed by the dust and re-emitted at the infrared wavelengths. However, these galaxies might have a quenched synchrotron radiation. This can be attributed to various reasons including a lack of supernovae remnants which accelerate particles producing radio emission, the escape of fast cosmic rays from the galaxy, etc. These two competing factors, dust and radio emission, counter balance each other (see Bell 2003). BCDs though, are typically small, less than $\sim 1\text{ kpc}$ in size, and have fewer HII regions with massive stars (w.r.t. normal galaxies) which heat the dust and go supernovae to produce cosmic rays. As a result the averaging effects in the sampling of the properties of the interstellar medium which result from the limited spatial resolution in dense galactic disks is not so prominent in BCDs. Furthermore, the small number of statistics may also contribute to the observed higher dispersion in q_{24} ratios in metal-poor dwarf galaxies. We investigate how metallicity affects the q_{24} ratios by dividing the dwarf galaxies in our sample into two groups: a lower metallicity group with $12 + \log(\text{O}/\text{H}) \leq 8.0$ and a higher metallicity group with $12 + \log(\text{O}/\text{H}) > 8.0$. This metallicity threshold was selected following Rosenberg et al. (2007) who noticed a change in the properties of the star-forming dwarf galaxies they studied around this metallicity value. We find

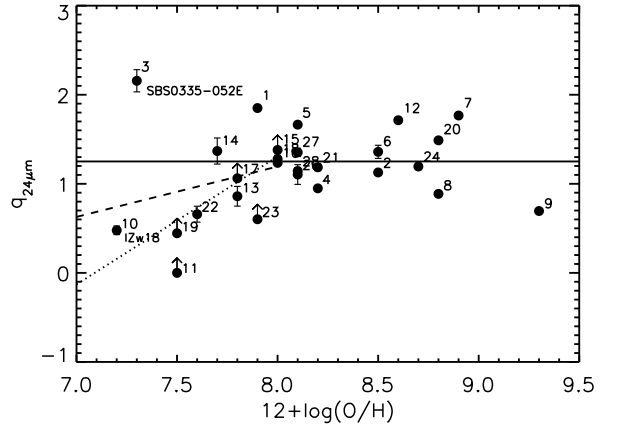


FIG. 3.— The q_{24} ratio plotted as a function of the oxygen abundance of the BCDs. The mean q_{24} value for all the sources is indicated by the solid line. A fit to the low metallicity sources ($12 + \log(\text{O}/\text{H}) \leq 8.0$) is indicated by the dashed line; while the dotted line is the same fit excluding SBS0335-052E.

a mean $q_{24} = 1.1 \pm 0.1$ ¹¹ for the first group and $q_{24} = 1.3 \pm 0.1$ for the second one. If we calculate the q_{24} for the low metallicity group without including SBS0335-052E, we find a much lower $q_{24} = 0.9 \pm 0.1$. We also notice that it appears q_{24} generally decreases with reduced metallicity for sources with $12 + \log(\text{O}/\text{H}) < 8.0$, with SBS035-052E as a clear outlier, and the slope flattens out at $12 + \log(\text{O}/\text{H}) > 8.0$ (see Fig. 3). This scatter in q_{24} at higher metallicities could be attributed to the more dispersion in the mid-IR emission in these sources and is consistent with a number of other studies that have found increased dispersion in the q ratios for very high luminosity galaxies (which usually have higher metallicities) (Condon et al. 1991; Yun et al. 2001; Bell 2003).

Hummel et al. (1988) have found evidence that, for a given galaxy, there is a small decrease in $F(100\mu\text{m})/S(20\text{cm})$ when the dust temperature increases. The latter can be traced by the ratio of $F(60\mu\text{m})/F(100\mu\text{m})$. Roussel et al. (2003) reached a similar result for the starburst galaxies they studied, in which they detected an anti-correlation of q_{FIR} with $F(60\mu\text{m})/F(100\mu\text{m})$. However, performing the same test for the q_{24} ratios on our dwarf galaxy sample which spans a range of flux ratios $-0.4 < \log(F(60\mu\text{m})/F(100\mu\text{m})) < 0.2$ we find no such clear trend. It is conceivable that this is partly because our sample is too small to identify a trend due to the intrinsic scatter in q_{24} .

3.3. Star Formation Rate Estimates

Both the radio and infrared emission can be used to estimate the star formation rates (SFRs) in galaxies. However, these correlations depend on a number of parameters including dust content, optical depth and metallicity. This topic and potential caveats have been discussed extensively in the literature (see Condon 1992; Kennicutt 1998, and references therein). For dwarf galaxies, the topic has been addressed in detail by Hopkins et al. (2002). The recent wealth of data from *Spitzer* has also

¹¹ Here we use the standard error of the mean (SEM) to quantify the dispersion in the mean value.

provided sufficient motivation to establish a calibration for the SFR using the infrared. Wu et al. (2005) and more recently Calzetti et al. (2007) have explored this topic using a large sample of star forming regions and nearby galaxies.

In Fig. 4 we plot the IR estimated SFR for our sample using the calibrations proposed by Wu et al. (2005) and Calzetti et al. (2007) respectively:

$$\text{SFR}_{24}(M_{\odot}\text{yr}^{-1}) = \frac{\nu L_{\nu}(24\mu\text{m})}{6.66 \times 10^8 L_{\odot}} \quad (1)$$

$$\text{SFR}_{24}(M_{\odot}\text{yr}^{-1}) = 1.27 \times 10^{-38} [L_{24}(\text{ergs}^{-1})]^{0.885} \quad (2)$$

as a function of the well-known radio to SFR formula of Condon (1992):

$$\text{SFR}_{1.4\text{GHz}} = 5.5 \times \frac{L_{1.4\text{GHz}}}{4.6 \times 10^{21} (\text{WHz}^{-1})} \quad (3)$$

The Wu et al. (2005) work is based on a global correlation without separating the low metallicity sources from metal rich galaxies. As can be seen in Fig. 4, a good agreement exists between the radio and IR estimated SFRs (indicated by diamonds). If we use the more recent calibration by Calzetti et al. (2007) on SFRs from $24\mu\text{m}$ luminosities, we find that most of the mid-IR estimated SFRs (marked as filled circles) are located below the 1:1 proportionality line, and thus they are consistently lower than both the SFRs estimated from the radio or from Wu et al. (2005). This is not unexpected since eq. 2 is calibrated based on the high metallicity sources that have significant $24\mu\text{m}$ emission, while most of our sources are metal-poor galaxies. We should also note that Calzetti et al. (2007) measure the SFR in individual HII regions in apertures within disks and subtract a “disk background”, which could partly explain the deviations we see from our analysis. These authors have also mentioned that the SFRs of low metallicity galaxies would be underestimated by a factor of 2–4 depending on how metal-poor the galaxies are. This deviation from a linear correlation is likely due to the lower opacities for decreasing metal content (Walter et al. 2007). When we fit the filled circles on Fig. 4, we find that $\log(\text{SFR}[\text{IR}]) = 0.94 \times \log(\text{SFR}[1.4\text{GHz}]/3.98)$, which is consistent with the metallicity correction factor suggested by Calzetti et al. (2007). We should stress once more though that as Bell (2003) has noted, the good agreement between the IR and radio estimates of SFRs does not necessarily mean that these are the “true” SFRs for the dwarf galaxies we study, but rather the competition of the lower dust content and suppressed synchrotron emission balances each other.

3.4. The Two Extremes: IZw18 and SBS0335-052E

Despite this overall agreement between the IR/radio correlation in our dwarf sample and the corresponding values of normal galaxies, the two lowest metallicity galaxies in our sample, IZw18 and SBS0335-052E, deviate markedly from the correlations and in opposite directions (see Fig. 3¹²). As the two most well-studied

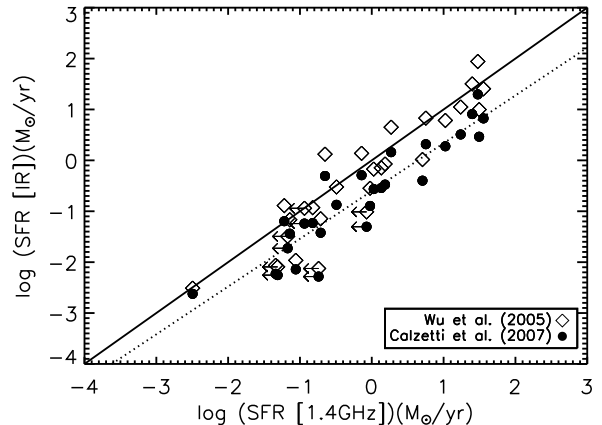


FIG. 4.— A plot of the SFR based on the $24\mu\text{m}$ luminosity as a function of the corresponding SFR estimated from the 1.4 GHz radio continuum emission for each galaxy in our sample. The open diamonds indicate the SFRs calculated using the $24\mu\text{m}$ fluxes following Wu et al. (2005) (eq.1), the filled circles are those using eq.2 from Calzetti et al. (2007). The solid line is the 1:1 proportionality line. The dotted line is a fit to the filled circles.

TABLE 3
COMPARISON OF SBS 0335-052E AND IZw 18

	SBS 0335-052E	IZw 18	Ratio ^a
12+log(O/H)	7.32	7.17	1.4
D (Mpc)	58	18	3
R (pc)	560 ^b	870 ^c	~0.6
SFR($M_{\odot}\text{yr}^{-1}$)	7×10^{-1}	5×10^{-2}	14
SNR(yr^{-1})	6×10^{-3}	2×10^{-4}	30
$L_{\text{H}\alpha}(L_{\odot})$	$5.6 \times 10^{7\text{d}}$	1.6×10^6	35
$L_{24\mu\text{m}}(L_{\odot})$	9×10^8	7×10^6	120
$L_{\text{IR}}(L_{\odot})$	$\sim 4 \times 10^9$	$\sim 4 \times 10^7$	100
$L_{1.4\text{GHz}}(\text{WHz}^{-1})$	2×10^{20}	8×10^{19}	2.5
M(Ks)(mag)	-18.3	-16.1	~80 ^e

^a Ratio of the relative quantities in SBS0335-052E to IZw18.

^b This is the size of the six super star clusters in SBS0335-052E, which has a size of $2''$ (Thuan et al. 1997). At a distance of 58 Mpc, $1'' \sim 280$ pc.

^c This indicate the largest projected linear extend of the total star-forming regions in this galaxy ($\sim 10''$, Hunt et al. 2005b). At a distance of 18 Mpc, $1'' \sim 87$ pc.

^d Flux in $1''$ slit multiplied by a factor of 2 to correct for aperture effects.

^e This is the approximate mass ratio of the two sources assuming that their mass scales with K-band luminosity and that both sources have the same M/L_{Ks} (see Bell & de Jong 2001).

BCDs, it is interesting to inspect the IR/radio properties of these two galaxies and a comparison of their physical parameters can be found in Table 3.

As indicated by the *Spitzer* IRS spectrum of SBS0335-052E (Houck et al. 2004b), the SED of the galaxy has an unusually flat mid-IR slope that peaks at $\sim 28\mu\text{m}$. Hunt et al. (2005a) used *DUSTY* models (Ivezić et al. 1999) to fit its SED and found a q_{FIR} value of 2.0 for this galaxy, lower than the typical q_{FIR} of ~ 2.3 expected for late type systems. These calculations are based on a 1.4GHz continuum flux of ~ 0.46 mJy, which corresponds

places it in a region of the plot where other sources with higher metallicity and higher luminosity are located.

¹² In Fig. 2 the “outlier” status of SBS0335-052E does not appear as prominent as in Fig. 3, because its high $24\mu\text{m}$ luminosity

to the compact part ($6''$) of SBS0335-052E (Dale et al. 2001; Hunt et al. 2004). Similarly, if we simply calculate the q ratio independent of any modelling work and only use the observable parameters, we find a $q_{70} = 2.1 \pm 0.1$ (assuming that the MIPS $70 \mu\text{m}$ flux density is $51.1 \pm 4.8 \text{ mJy}$, Engelbracht et al. 2007). This is in good agreement with the $q_{70} = 2.16 \pm 0.17$ for the sources in the First Look Survey studied by Appleton et al. (2004).

However, when we examine the q_{24} for SBS0335-052E, adopting a MIPS $24 \mu\text{m}$ flux of 66 mJy , we find a q_{24} ratio of 2.2 ± 0.1 . We see a 2σ excess in the q parameter compared with the mean q_{24} of 1.3 ± 0.4 in the dwarf sample. If this excess is real, it would be consistent with the unique shape of the SED of the galaxy, which suggests that the dust grain distribution is dominated by small grains with temperatures of $\sim 150 \text{ K}$ and a total dust mass of $\sim 10^3 M_{\odot}$ (Houck et al. 2004b). Whether the large grains were never created or they were destroyed by shocks is unknown. The elevated q_{24} ratio could also be due to the lack of synchrotron emission. Roussel et al. (2003, 2006) have shown their study of three starburst galaxies, all of which have q_{FIR} more than 3σ higher the mean q_{FIR} and categorized them to be nascent starbursts. SBS0335-052E though, could also be a candidate of this group. It is based partly on the high q_{24} value, as well as its low $\text{H}\alpha$ luminosity as compared to the infrared or radio luminosities (see Table 3). Finally, Hunt et al. (2004) have shown the existence of free-free absorption in the radio spectrum of SBS0335-052E, which is usually caused by young, dense and heavily embedded clusters¹³.

IZw18, despite its similar metallicity to SBS0335-052E ($12 + \log(\text{O}/\text{H}) = 7.17$ and 7.32 respectively), shows a rather different q ratio. It also has an IR luminosity of $L_{\text{IR}} \sim 10^7 L_{\odot}$, just 1% of the L_{IR} in SBS0335-052E. In low luminosity galaxies, radio emission is known to decrease faster than dust emission (Devereux & Eales 1989), and high IR/radio ratios have been observed in low luminosity dwarf galaxies (Klein et al. 1984). In IZw18 though, we find a rather low infrared to radio ratio. The q_{24} is found to be 0.5 ± 0.1 , nearly 2σ lower than the average value of our sample. At longer wavelengths, IZw18 is faint and no *IRAS* FIR data are available. However, as noted by Wu et al. (2007a) (see their Fig. 5), it has a very similar $5\text{--}38 \mu\text{m}$ continuum slope to the typical starburst galaxy NGC7714 (Brandl et al. 2004). If we were to assume that this similarity extends to the FIR and scale down the *IRAS* 60 and $100 \mu\text{m}$ flux densities of NGC7714 by a factor of 375 so that its corresponding $22 \mu\text{m}$ flux density matches the one of IZw18, we find its “equivalent” *IRAS* 60 and $100 \mu\text{m}$ flux density to be 29.8 and 32.8 mJy respectively. This would result in q_{FIR} of 1.3 for the galaxy, which deviates from the average q_{FIR} ratio of 2.3 ± 0.2 calibrated by Condon (1992) by nearly 5σ . If we were to use the MIPS $70 \mu\text{m}$ detection of 34 mJy for IZw18 (Engelbracht et al. 2007) and calculate its q ratio, we would find $q_{70} = 1.4$, again 5σ away from the average q_{70} suggested by Appleton et al. (2004).

A number of plausible scenarios were considered to explain this result, though none appears convincing. As

discussed in Wu et al. (2007a), because the optical depth of IZw18 is small, it could be that a significant fraction of the UV light has leaked out without being absorbed by the dust, thus resulting in a damped $24 \mu\text{m}$ emission. Alternatively, IZw18 may simply have an unusually high radio luminosity at 1.4 GHz . Could it be that IZw18 is observed at a special moment right after the explosion of a supernovae event? Radio supernovae fade by more than a factor of 10 within $\sim 3 \text{ yr}$ (Chevalier 1982). The radio continuum observations of IZw18 span over a period of more than 5 yrs (Hunt et al. 2005b; Cannon et al. 2005) but show no variation, thus this is not likely.

The recent results by Murphy et al. (2006b) provide another possible scenario. These authors analyzed a sample of nearby spiral galaxies and found that systems with higher disk-averaged SFRs (Σ_{SFR}) have usually experienced a recent episode of enhanced star formation. As a result they contain a higher fraction of young cosmic ray electrons that have traveled only a few hundred parsecs from their acceleration sites in supernova remnants. This is perhaps the case for IZw18. However, other sources in our sample also have elevated Σ_{SFR} and show no radio excess. It could also be that the extremely low metal abundance of IZw18, 0.15 dex lower than that of SBS0335-052E, is below a critical threshold. The newly formed stars in the unpolluted interstellar medium may produce, and subsequently heat, less dust than electrons which are accelerated and contribute in the radio emission. We also note that the rate of SNR in IZw18 is a factor of ~ 30 lower than that in SBS0335-052E (see Table 3) but its morphology is much more disturbed with filamentary structure and outflows (see Izotov & Thuan 2004). If we were to assume that both sources have similar mass-to-light ratios and estimate their mass from their K-band luminosities, we find that the mass of IZw18 is almost a factor of 80 less than that of SBS0335-052E. Thus the rate of SNR normalized with mass in IZw18 would be ~ 2.5 times that of SBS0335-052E. Could it be that the disturbed morphology of IZw18 in addition to its low metal content that it created the conditions in the interstellar medium for this abnormally high radio flux? The question remains open.

4. CONCLUSIONS

We have studied the mid-IR and FIR to radio correlation in a sample of dwarf star-forming galaxies spanning a metallicity range from $7.2 < 12 + \log(\text{O}/\text{H}) < 8.9$, using *Spitzer* IRS/MIPS, as well as radio 1.4 GHz data obtained from the literature. The BCD sample appears to follow the same FIR/radio correlation as normal star forming galaxies. The analysis based on mid-IR and radio data reveals a similar correlation, though the scatter is larger, probably due to an intrinsically higher variation in the $15\text{--}30 \mu\text{m}$ SEDs of dwarf galaxies. When comparing the q_{24} ratios with metallicity or effective dust temperature, we find no strong correlation, though there is a general trend of lower q ratios at lower metallicity for galaxies with $12 + \log(\text{O}/\text{H}) < 8.0$ and the correlation flattens out toward higher metallicity. In general the SFRs estimated from the radio 1.4 GHz continuum and the mid-IR data are in good agreement. Two extremely metal poor BCDs, IZw18 and SBS0335-052E appear to deviate from the average q_{24} by $\sim 2\sigma$, with one displaying a radio excess and the other an infrared excess.

¹³ Note, that if we could properly account for the self-absorption of the radio continuum, the intrinsic q ratio would decrease. However, the exact fraction for absorption is not known and more data at $\nu < 1.5 \text{ GHz}$ would be needed to determine that number.

The authors would like to thank P. Appleton and D. Calzetti for stimulating discussions. We would also like to thank G. Helou, L.K. Hunt as well as an anonymous referee whose detailed comments and insightful suggestions have helped to improve this manuscript. This work is based in part on observations made with the *Spitzer*

Space Telescope, which is operated by the Jet Propulsion Laboratory, California Institute of Technology, under NASA contract 1407. Support for this work was provided by NASA through Contract Number 1257184 issued by JPL/Caltech. VC would like to acknowledge the partial support from the EU ToK grant 39965.

REFERENCES

- Allende Prieto, C., Lambert, D. L., & Asplund, M. 2001, *ApJ*, 556, L63
- Aloisi, A. et al. 2007, *ApJ*, 667, L151
- Appleton, P. N., et al. 2004, *ApJS*, 154, 147
- Becker, R. H., White, R. L., & Helfand, D. J. 1995, *ApJ*, 450, 559
- Bell, E. F., & de Jong, R. S. 2001, *ApJ*, 550, 212
- Bell, E. F. 2003, *ApJ*, 586, 794
- Bergvall, N., & Östlin, G. 2002, *A&A*, 390, 891
- Brandl, B. R., et al. 2004, *ApJS*, 154, 188
- Brandl, B. R., et al. 2006, *ApJ*, 653, 1129
- Boyle, B. J., Cornwell, T. J., Middelberg, E., Norris, R. P., Appleton, P. N., & Smail, I. 2007, *MNRAS*, 376, 1182
- Calzetti, D., et al. *ApJ*, 666,870
- Cannon, J. M., Walter, F., Skillman, E. D., & van Zee, L. 2005, *ApJ*, 621, L21
- Chevalier, R. A. 1982, *ApJ*, 258, 790
- Condon, J. J., Anderson, M. L., & Helou, G. 1991, *ApJ*, 376, 95
- Condon, J. J. 1992, *ARA&A*, 30, 575
- Condon, J. J., Cotton, W. D., Greisen, E. W., Yin, Q. F., Perley, R. A., Taylor, G. B., & Broderick, J. J. 1998, *AJ*, 115, 1693
- Dale, D. A., Helou, G., Neugebauer, G., Soifer, B. T., Frayer, D. T., & Condon, J. J. 2001, *AJ*, 122, 1736
- Dale, D. A., et al. 2006, *ApJ*, 646, 161
- de Jong, T., Klein, U., Wielebinski, R., & Wunderlich, E. 1985, *A&A*, 147, L6
- Devereux, N. A., & Eales, S. A. 1989, *ApJ*, 340, 708
- Elbaz, D., Cesarsky, C. J., Chantal, P., Aussel, H., Franceschini, A., Fadda, D., & Chary, R. R. 2002, *A&A*, 384, 848
- Engelbracht, C. W., Gordon, K. D., Rieke, G. H., Werner, M. W., Dale, D. A., & Latter, W. B. 2005, *ApJ*, 628, L29
- Engelbracht, C. W., et al. 2007, *ApJ*, submitted
- Garrett, M. A. 2002, *A&A*, 384, L19
- Grupponi, C., Pozzi, F., Zamorani, G., Ciliegi, P., Lari, C., Calabrese, E., La Franca, F., & Matute, I. 2003, *MNRAS*, 341, L1
- Guseva, N. G., Izotov, Y. I., & Thuan, T. X. 2000, *ApJ*, 531, 776
- Hao, Lei, et al., 2007, in preparation
- Harwit, M., & Pacini, F. 1975, *ApJ*, 200, L127
- Heckman, T. M., Robert, C., Leitherer, C., Garnett, D. R., & van der Rydt, F. 1998, *ApJ*, 503, 646
- Helou, G., Soifer, B. T., & Rowan-Robinson, M. 1985, *ApJ*, 298, L7
- Helou, G., & Bica, M. D. 1993, *ApJ*, 415, 93
- Hopkins, A. M., Schulte-Ladbeck, R. E., & Drozdovsky, I. O. 2002, *AJ*, 124, 862
- Houck, J. R., et al. 2004a, *ApJS*, 154, 18
- Houck, J. R., et al. 2004b, *ApJS*, 154, 211
- Hummel, E., Davies, R. D., Pedlar, A., Wolstencroft, R. D., & van der Hulst, J. M. 1988, *A&A*, 199, 91
- Hunt, L. K., Dyer, K. K., Thuan, T. X., & Ulvestad, J. S. 2004, *ApJ*, 606, 853
- Hunt, L., Bianchi, S., & Maiolino, R. 2005b, *A&A*, 434, 849
- Hunt, L. K., Dyer, K. K., & Thuan, T. X. 2005a, *A&A*, 436, 837
- Izotov, Y. I., & Thuan, T. X. 2004, *ApJ*, 616, 768
- Izotov, Y. I., & Thuan, T. X. 1998, *ApJ*, 500, 188
- Izotov, Y. I., & Thuan, T. X. 1999, *ApJ*, 511, 639
- Ivezić, Z., Nenkova, M., & Elitzur, M. 1999, User Manual for *DUSTY*, University of Kentucky Internal Report, accessible at <http://www.pa.uky.edu/~moshe/dusty>
- Jannuzi, B. T., & Dey, A. 1999, *ASP Conf. Ser.* 191: Photometric Redshifts and the Detection of High Redshift Galaxies, 111
- Kennicutt, R. C., Jr. 1998, *ARA&A*, 36, 189
- Kirshner, R. P., Oemler, A., Jr., Schechter, P. L., & Shectman, S. A. 1981, *ApJ*, 248, L57
- Klein, U., Weiland, H., & Brinks, E. 1991, *A&A*, 246, 323
- Klein, U., Wielebinski, R., & Thuan, T. X. 1984, *A&A*, 141, 241
- Kobulnicky, H. A., & Skillman, E. D. 1997, *ApJ*, 489, 636
- Kobulnicky, H. A., & Johnson, K. E. 1999, *ApJ*, 527, 154
- Kunth, D., & Joubert, M. 1985, *A&A*, 142, 411
- Leroy, A., Bolatto, A. D., Simon, J. D., & Blitz, L. 2005, *ApJ*, 625, 763
- Miller, N. A., & Owen, F. N. 2001, *AJ*, 121, 1903
- Moshir, M., et al. 1990, *IRAS Faint Source Catalogue*, version 2.0 (1990)
- Moustakas, J., & Kennicutt, R. C., Jr. 2006, *ApJS*, 164, 81
- Murphy, E. J., et al. 2006a, *ApJ*, 638, 157
- Murphy, E. J., et al. 2006b, *ApJ*, 651, L111
- Popescu, C. C., & Hopp, U. 2000, *A&AS*, 142, 247
- Rieke, G. H., et al. 2004, *ApJS*, 154, 25
- Rosenberg, J. L., Ashby, M. L. N., Salzer, J. J., & Huang, J.-S. 2006, *ApJ*, 636, 742
- Rosenberg, J. L., Wu, Yanling, Le Floc'h, E., Charmandaris, V., Ashby, M. L. N., Houck, J. R., Salzer, J. J. Willner, S.P. 2008, *ApJ*, in press, astro-ph/0710.5514
- Roussel, H., Helou, G., Beck, R., Condon, J. J., Bosma, A., Matthews, K., & Jarrett, T. H. 2003, *ApJ*, 593, 733
- Roussel, H., et al. 2006, *ApJ*, 646, 841
- Sanders, D. B., Mazzarella, J. M., Kim, D.-C., Surace, J. A., & Soifer, B. T. 2003, *AJ*, 126, 1607
- Sanders, D. B., et al. 2007, *ApJS*, (in press arXiv:astro-ph/0701318)
- Shi, F., Kong, X., Li, C., & Cheng, F. Z. 2005, *A&A*, 437, 849
- Storchi-Bergmann, T., Calzetti, D., & Kinney, A. L. 1994, *ApJ*, 429, 572
- Thuan, T. X., & Izotov, Y. I. 2005, *ApJS*, 161, 240
- Thuan, T. X., Izotov, Y. I., & Lipovetsky, V. A. 1997, *ApJ*, 477, 661
- van der Kruit, P. C. 1971, *A&A*, 15, 110
- Walter, F., et al. 2007, *ApJ*, 661, 102
- Werner, M. W., et al. 2004, *ApJS*, 154, 1
- Wu, H., Cao, C., Hao, C.-N., Liu, F.-S., Wang, J.-L., Xia, X.-Y., Deng, Z.-G., & Young, C. K.-S. 2005, *ApJ*, 632, L79
- Wu, Y., Charmandaris, V., Hao, L., Brandl, B. R., Bernard-Salas, J., Spoon, H. W. W., & Houck, J. R. 2006, *ApJ*, 639, 157
- Wu, Y., et al., 2007a, *ApJ*, 662, 952
- Wu, Y., Bernard-Salas, J., Charmandaris, V., Leboutteiller, V., Hao, L., Brandl, B.R., Houck, J.R. 2007b, *ApJ* in press, astro-ph/0710.0003
- Yun, M. S., Reddy, N. A., & Condon, J. J. 2001, *ApJ*, 554, 803